Supporting Information

Highly efficient direct oxygen electro-reduction by partially unfolded laccases immobilized on waste-derived magnetically separable nanoparticles

Daily Rodríguez-Padrón[a], Alain R. Puente-Santiago[a]*, Alvaro Caballero[b], Alina M. Balu[a], Antonio A. Romero, Rafael Luque[a]*

[a]*Departamento de Química Orgánica, Grupo FQM-383, Universidad de Cordoba, Campus de Rabanales, Edificio Marie Curie (C-3), Ctra Nnal IV-A, Km 396, E14014, Cordoba (Spain), e-mail: q62alsor@uco.es, apuentesantiago@gmail.com*

[b]*Departamento de Química Inorgánica e Ingeniería Química, Campus de Rabanales, Edificio Marie Curie (C-3), Ctra Nnal IV-A, Km 396, E14014, Cordoba*

Abstract

A biocatalytic system based on laccase functionalized iron oxide nanoparticles (LAC-DA-Fe_2O_3) was designed by a mechanochemical approach and applied to the electrocatalytic reduction of oxygen. The full characterization of the obtained bioconjugates was performed; in particular, the spectroscopy characterization by UV-vis and FT-IR revealed that the protein adopted a partially unfolded state. The mentioned configuration, together with the geometry coordination changes along the T1 center can be further related to a high bioelectrocatalytic response. A current density up to 2.9 mA/cm^2 has been achieved, which is among the highest values reported in the literature for laccase functionalized nanomaterials.

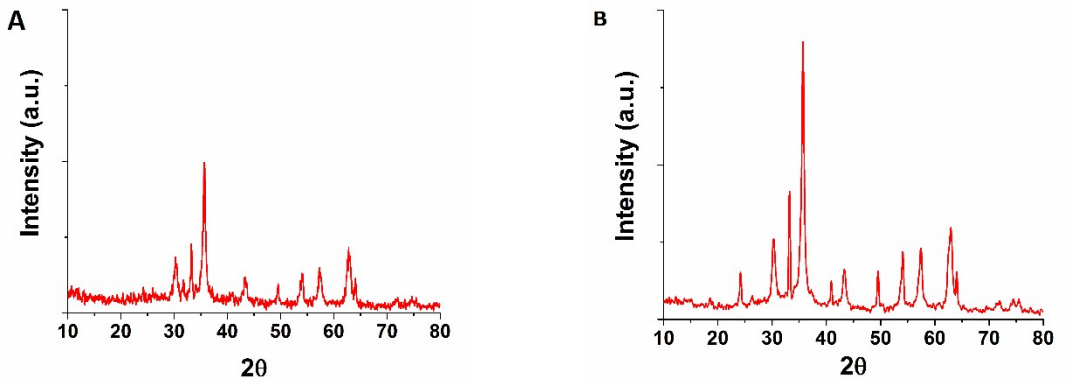

Figure S1. X-ray diffraction patterns of A: LAC-DA-Fe_2O_3 and B: Fe_2O_3.

Table S1. Magnetic susceptibility of the Fe_2O_3 and LAC-DA-Fe_2O_3.

Material	**Magnetic susceptibility (10^{-6} m^3Kg^{-1})**
Fe_2O_3	250
LAC-DA-Fe_2O_3	236

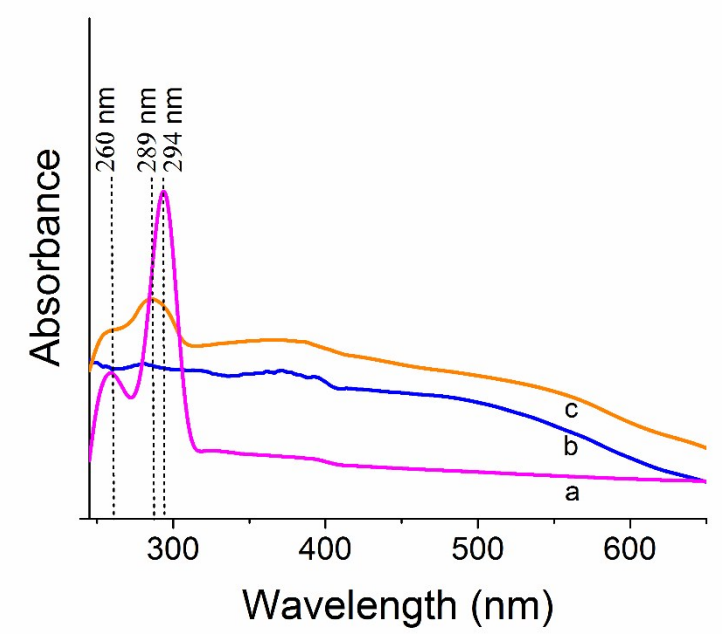

Figure S2. UV-vis spectra for DA-Fe_2O_3 (orange line), Fe_2O_3 (blue line) and DA (pink line).

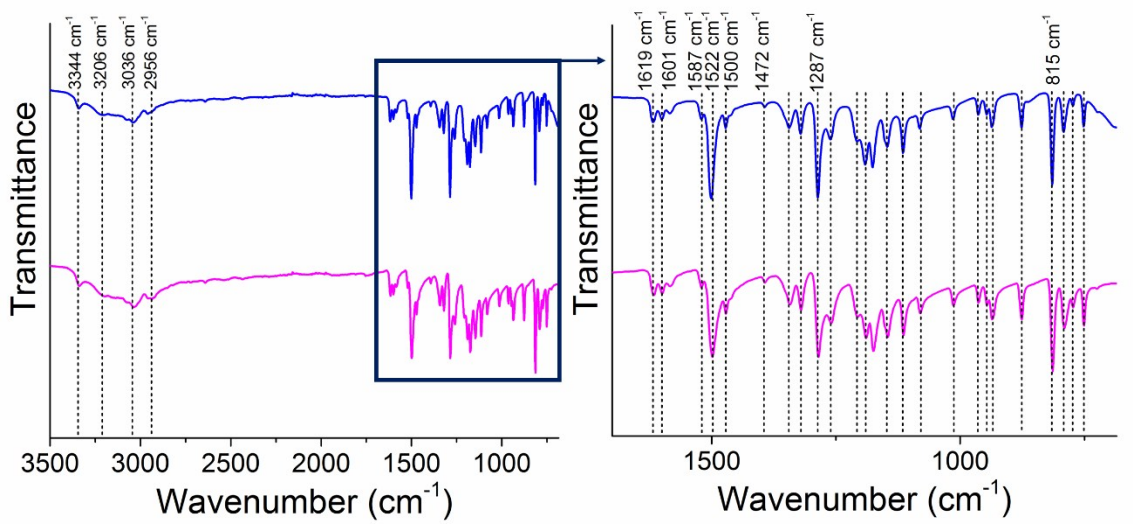

Figure S3. FT-IR spectra for DA-Fe_2O_3 (pink line) and commercial DA (blue line).

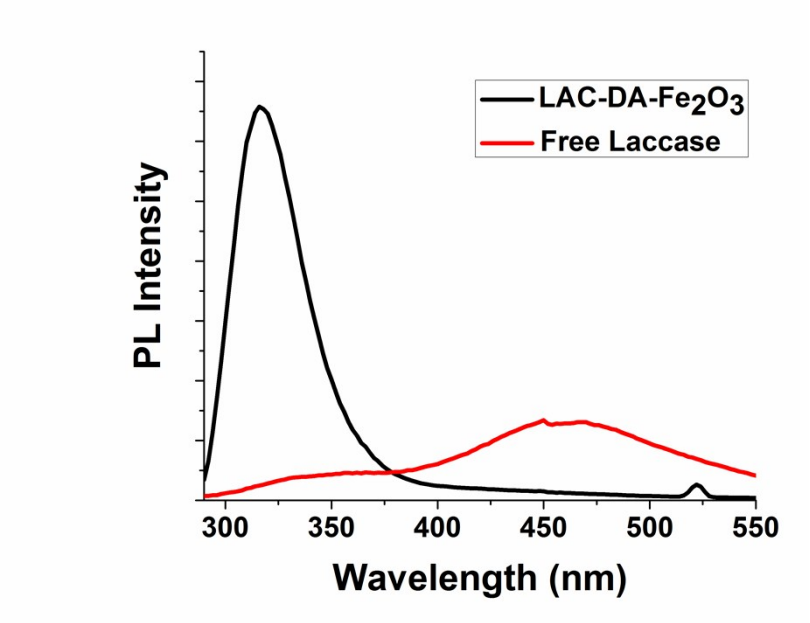

Figure S4. Fluorescence emission spectra of LAC-DA-Fe_2O_3 nanobioconjugates (black line) and free laccase from Aspergillus sp. (red line). Excitation wavelength = 260 nm.

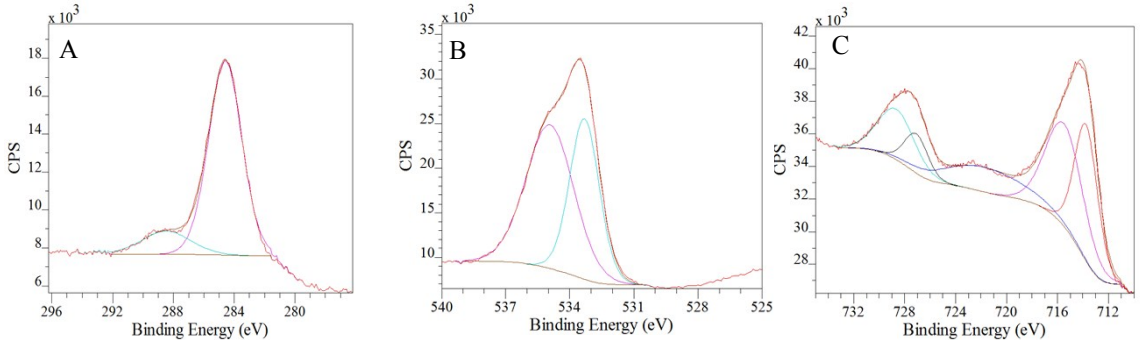

Figure S5. Deconvoluted high-resolution XPS spectra of Fe_2O_3 for a) C 1s, b) O 1s and c) Fe 2p.

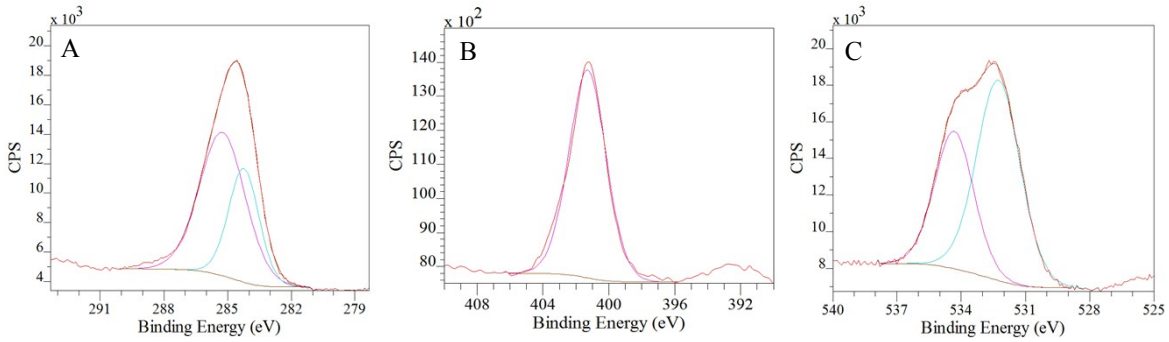

Figure S6. Deconvoluted high-resolution XPS spectra of DA-Fe_2O_3 for a) C 1s, b) N 1s and c) O 1s.

Table S2. Components quantification in the C1s, N1s and O1s XPS regions.

Material	**C-C (%)**	**C-N (%)**	**C-O (%)**
LAC-DA-Fe_2O_3	50.3	44.2	5.5
	$N_{PEPTIDE\ BONDS}$ (%)	**$N_{PIRIMIDINIC\ GROUPS}$ (%)**	
	50.3	44.2	
	O-C (%)	**O-Fe (%)**	
	57.5	42.5	

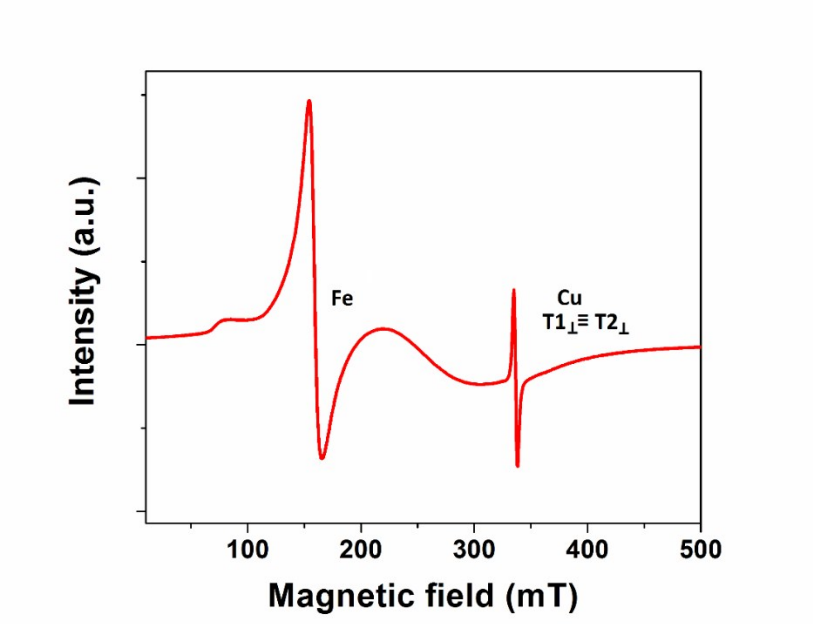

Figure S7. EPR spectra of LAC-DA-Fe_2O_3 nanobioconjugates.

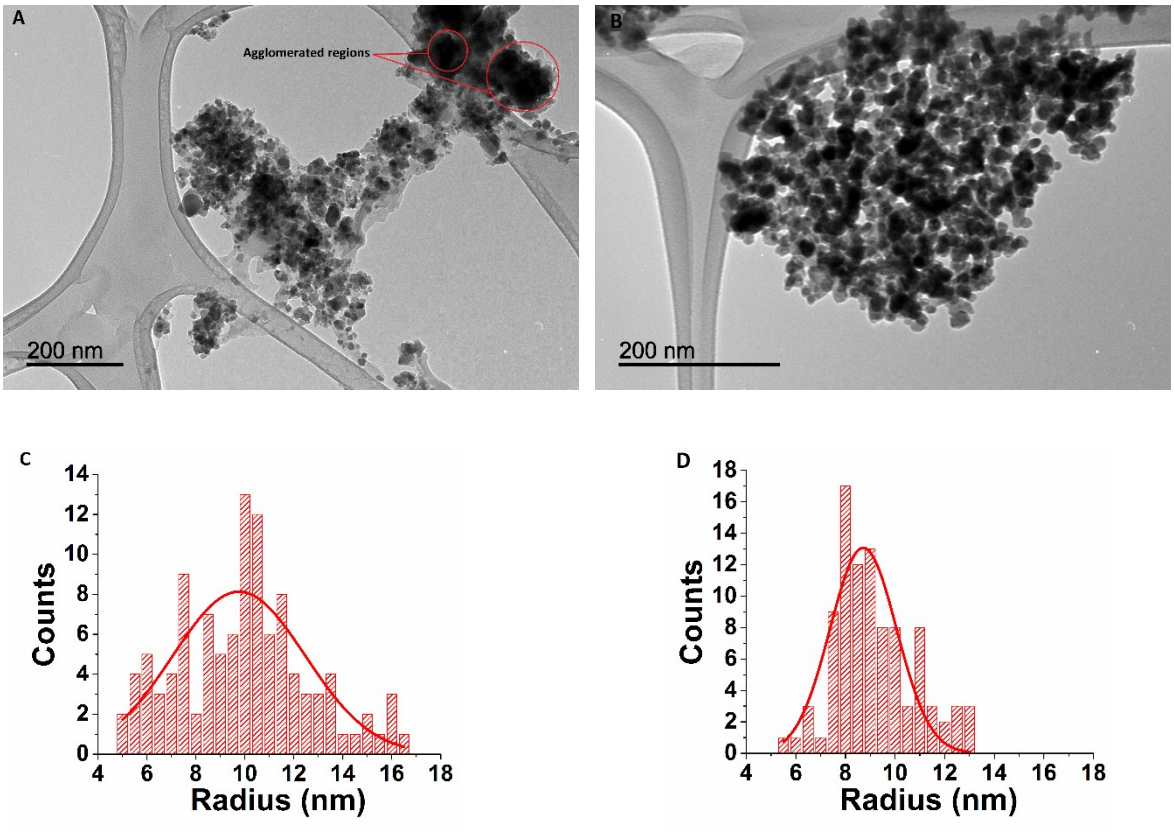

Figure S8. TEM image of the A: LAC-DA-Fe_2O_3 and B: Fe_2O_3 nanoparticles. Size distribution based on TEM of C: LAC-DA-Fe_2O_3 (100 particles) and D: Fe_2O_3 (100 particles).

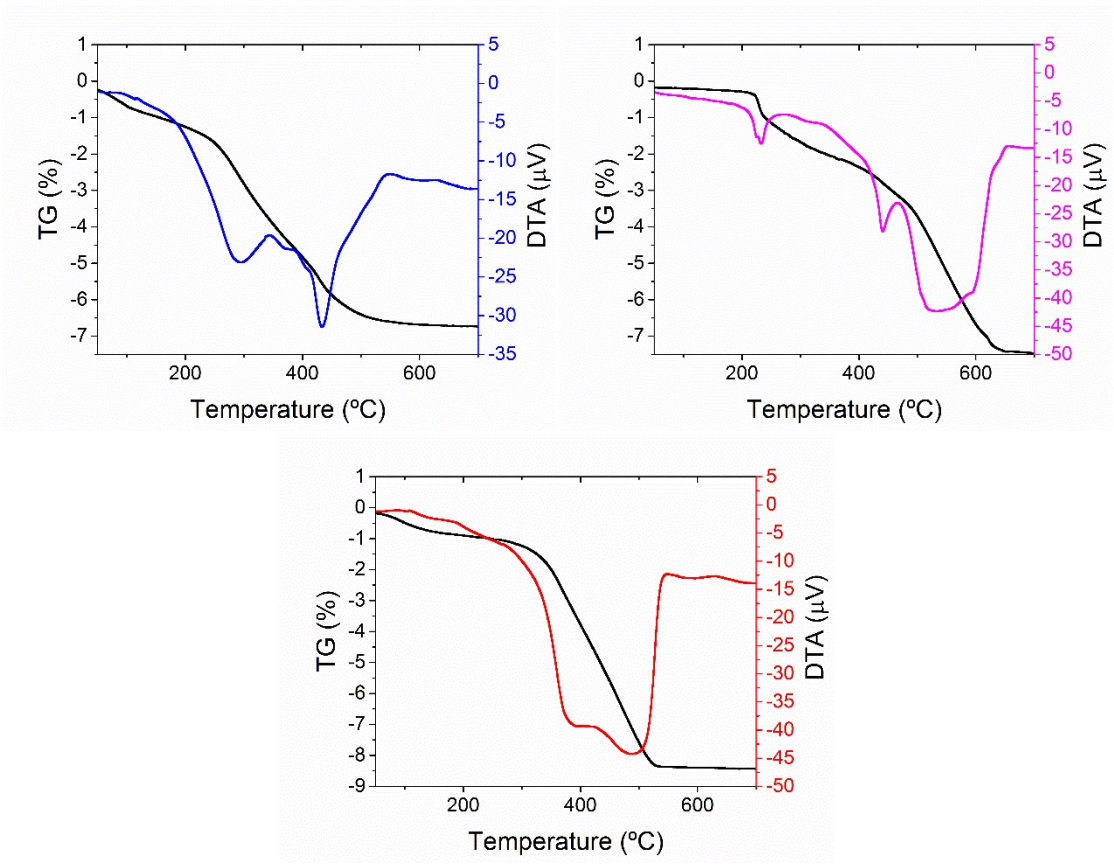

Figure S9. TG-DTA of LAC-DA-Fe_2O_3 (blue line), DA-Fe_2O_3 (pink line), Fe_2O_3 (red line) nanomaterials.

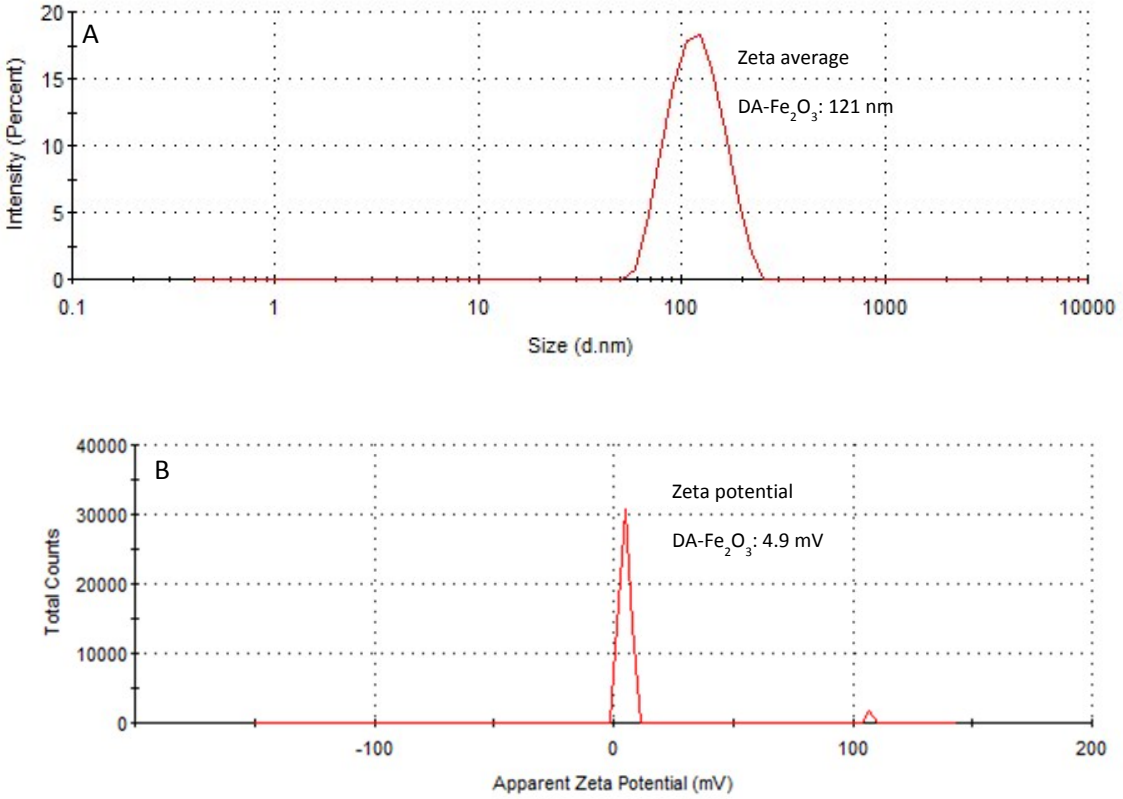

Figure S10. A. Dynamic light scattering data and **B.** zeta potential of DA-Fe_2O_3.

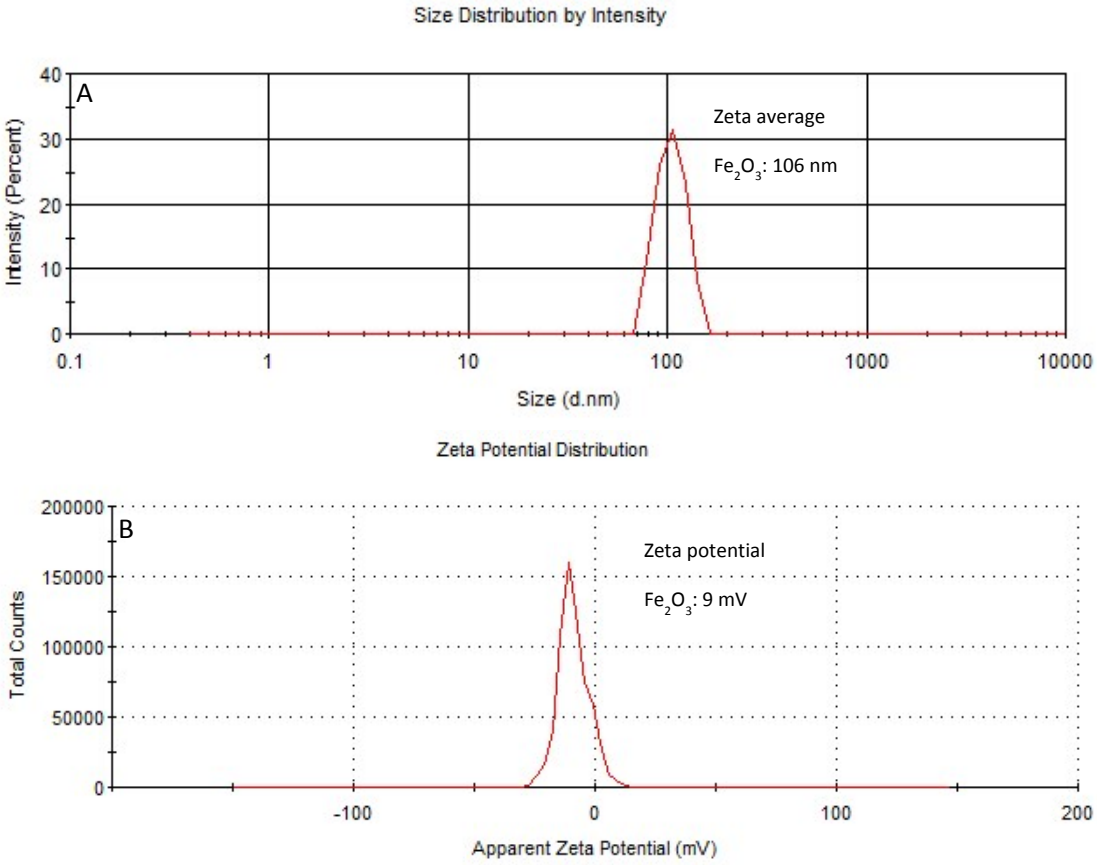

Figure S11. A. Dynamic light scattering data and **B.** zeta potential of Fe_2O_3.